INSTITUTO DE CIENCIAS FÍSICAS

SEXTEN CENTER FOR ASTROPHYSICS RICCARDO GIACCONI

Computing the three-point correlation functions in photometric galaxy surveys

Sofia del Pilar Samario-Nava
ssamario@icf.unam.mx

Supervisors:
Dr. Alejandro Aviles
Dr. Juan Carlos Hidalgo

Modeling the 3-point correlation function of projected scalar fields on the sphere

Abraham Arvizu[a,b] **Alejandro Aviles**[b] **Juan Carlos Hidalgo**[b] **Eladio Moreno**[a] **Gustavo Niz**[a] **Mario A. Rodriguez-Meza**[c] **Sofía Samario**[b] **The LSST Dark Energy Science Collaboration**

[a]Departamento de Ciencias e Ingenierias, Universidad de Guanajuato, 37150, León, Guanajuato

[b]Instituto de Ciencias Físicas, Universidad Nacional Autónoma de México, 62210, Cuernavaca, Morelos.

[c]Departamento de Física, Instituto Nacional de Investigaciones Nucleares, Apartado Postal 18-1027, Col. Escandón, Ciudad de México,11801, México.

2408.16847

2506.19811

Non-Gaussian statistics in galaxy weak lensing: compressed three-point correlations and cosmological forecasts

Sofia Samario-Nava[a] **Alejandro Aviles**[a] **Juan Carlos Hidalgo**[a]

[a]Instituto de Ciencias Físicas, Universidad Nacional Autónoma de México, 62210, Cuernavaca, Morelos.

Motivation

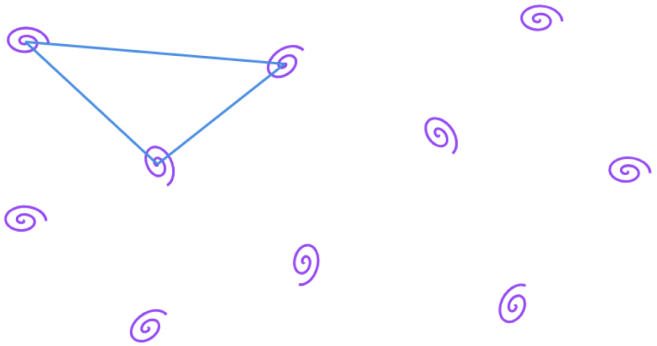

$$N \times (N-1) \times (N-2) \sim \mathcal{O}(N^3)$$

$$N \sim 10^8$$

$$N^3 \sim 10^{24}$$

Motivation

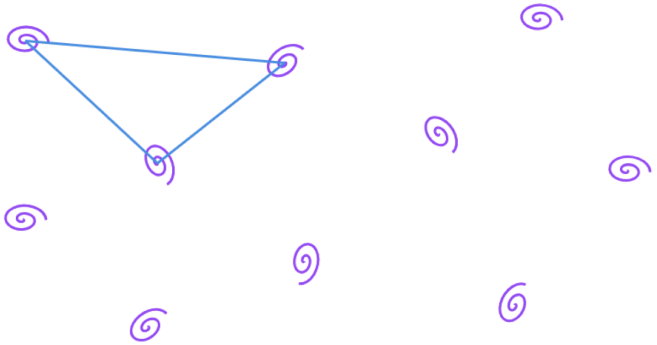

$$N \times (N-1) \times (N-2) \sim \mathcal{O}(N^3)$$

$$N \sim 10^8$$

$$N^3 \sim 10^{24}$$

$$\zeta(\theta_1, \theta_2, \phi) = \sum_{n=-\infty}^{\infty} \zeta_n(\theta_1, \theta_2) e^{in\phi},$$

$$N^2 \sim 10^{16} \longrightarrow N \log N$$

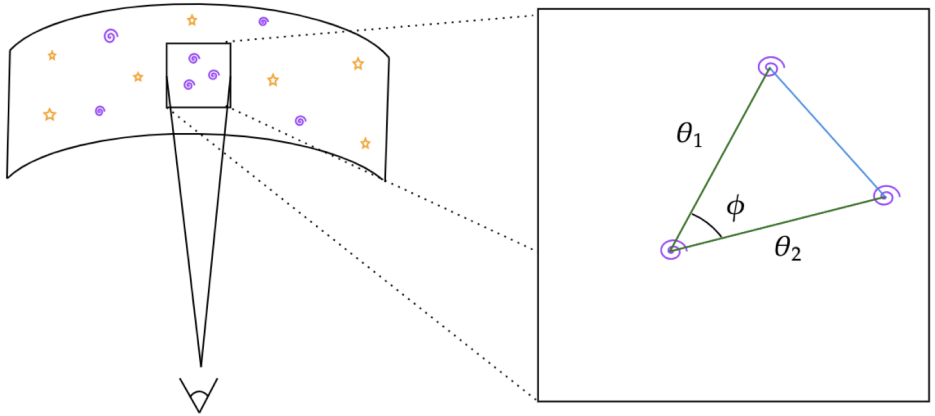

Weak lensing

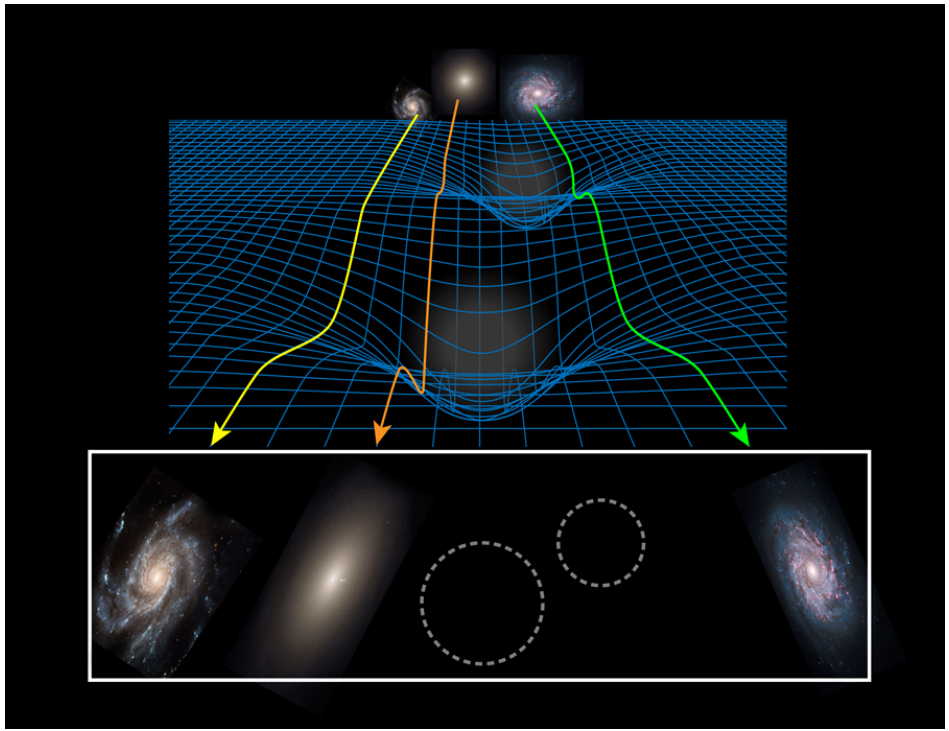

APS/Alan Stonebraker; galaxy images from STScI/AURA, NASA, ESA, and the Hubble Heritage Team

$$\zeta(\theta_1, \theta_2, \phi) = \sum_{n=-\infty}^{\infty} \zeta_n(\theta_1, \theta_2) e^{in\phi},$$

$$\xi_+ + \zeta_0$$

$$\xi_+ + \zeta_0 + \zeta_1$$

$$\xi_+ + \zeta_0 + \zeta_1 + \ldots + \zeta_i$$

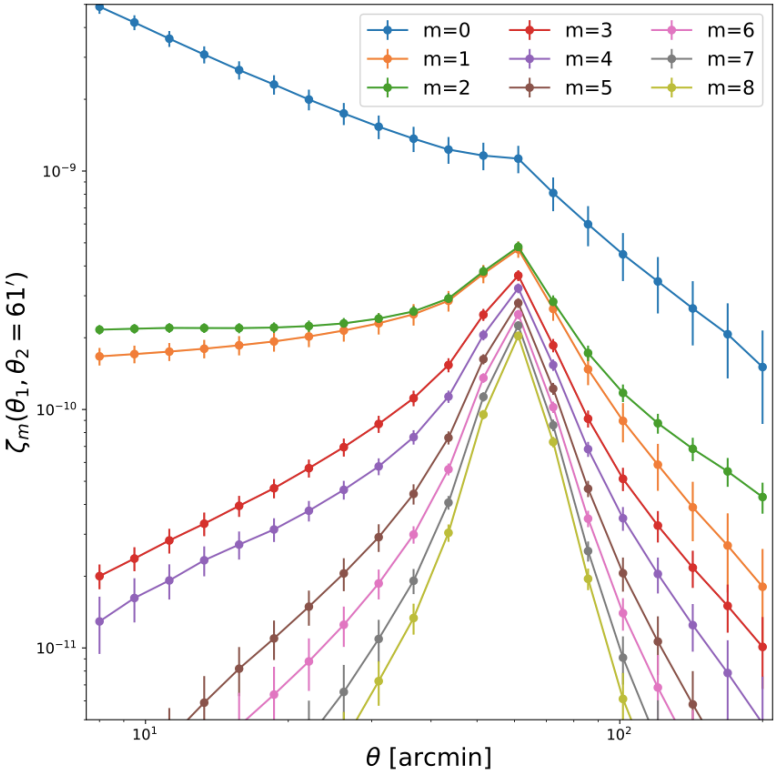

Covariance matrix

Estimator

Signal modeling

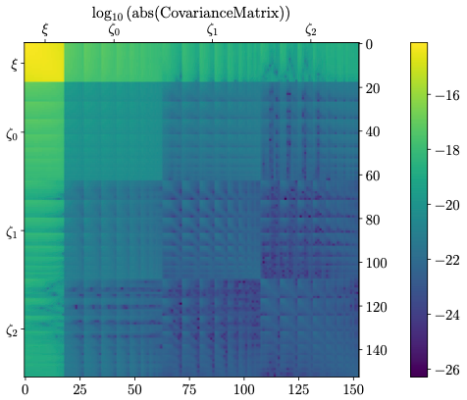

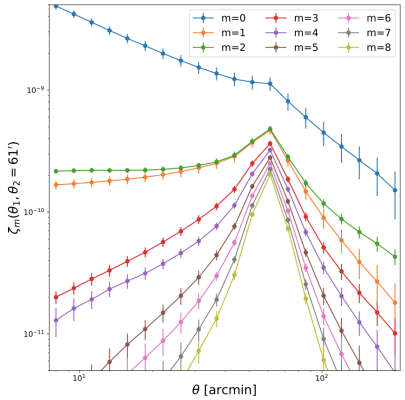

2408.16847

$$B(\ell_1, \ell_2, \varphi) = \sum_{m=-\infty}^{\infty} B_m(\ell_1, \ell_2) e^{im\varphi}$$

$$\zeta_m(\theta_1, \theta_2) = (-1)^m \int \frac{\ell_1 d\ell_1 \ell_2 d\ell_2}{(2\pi)^2} J_m(\ell_1\theta_1) J_m(\ell_2\theta_2) B_m(\ell_1, \ell_2)$$

Fisher Forecast

$$\xi_+ + \zeta_0 \qquad \xi_+ + \zeta_0 + \zeta_1 \qquad \xi_+ + \zeta_0 + \zeta_1 + \ldots + \zeta_i$$

Cosmological Forecast per multipole

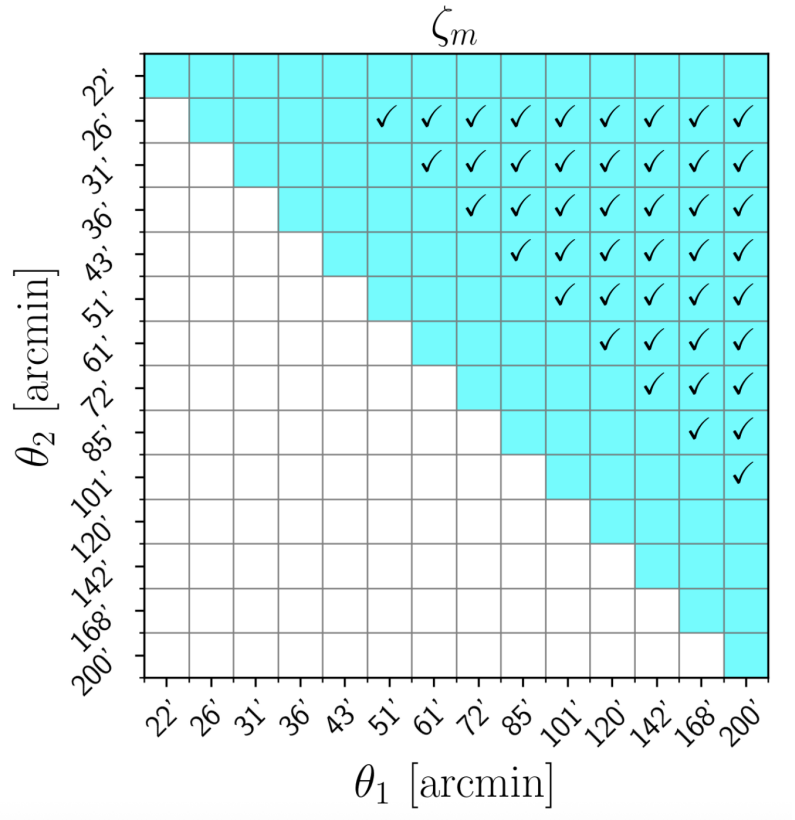
ζ_m
θ_2 [arcmin]
22'
26'
31'
36'
43'
51'
61'
72'
85'
101'
120'
142'
168'
200'
θ_1 [arcmin]

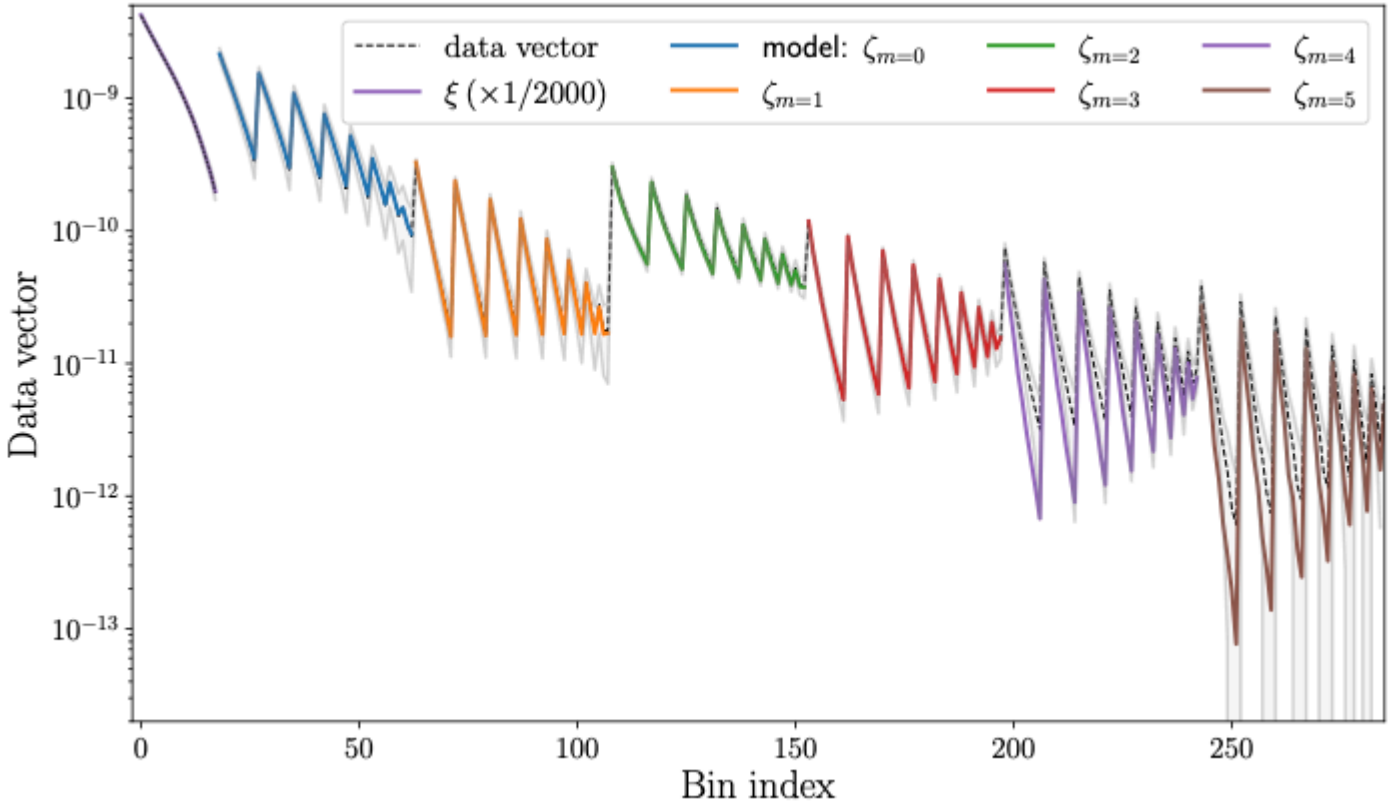
data vector
ξ (×1/2000)
model: $\zeta_{m=0}$
$\zeta_{m=1}$
$\zeta_{m=2}$
$\zeta_{m=3}$
$\zeta_{m=4}$
$\zeta_{m=5}$
Data vector
10^{-9}
10^{-10}
10^{-11}
10^{-12}
10^{-13}
0
50
100
150
200
250
Bin index

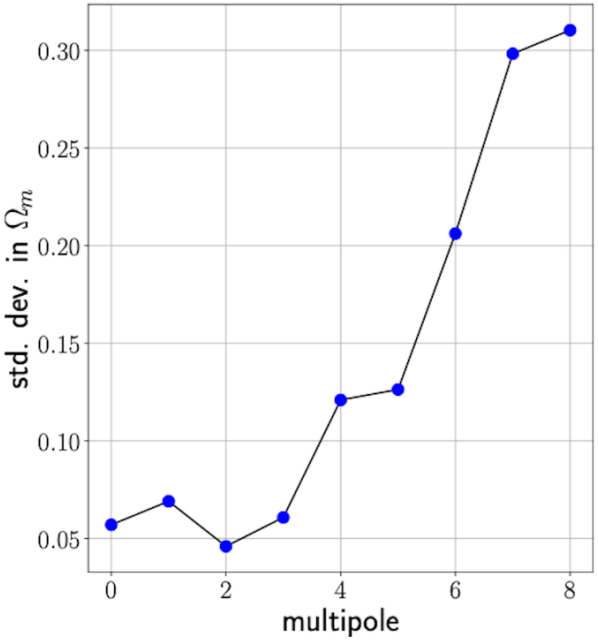

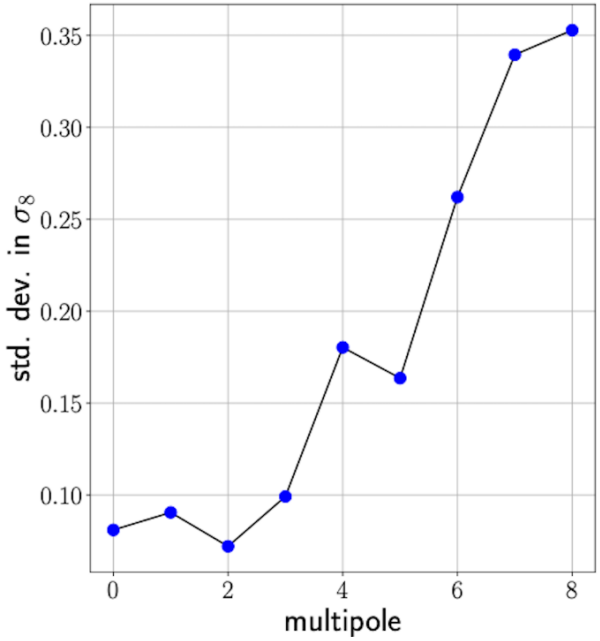

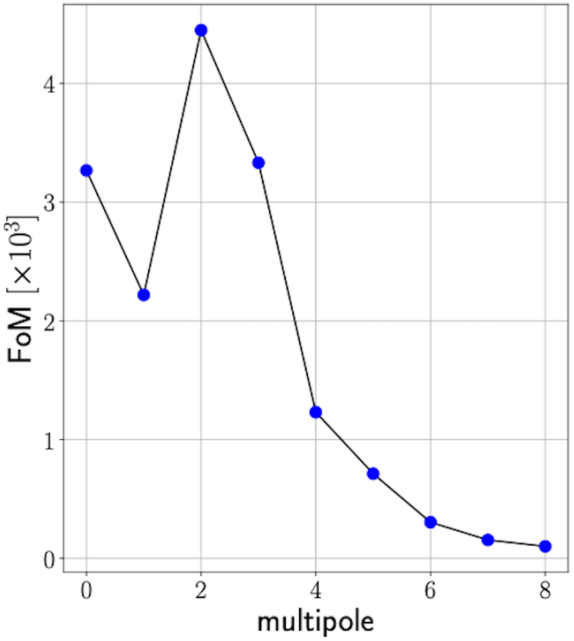

This plot shows the quadrupole is the multipole providing the most restrictive constraints, with $\sqrt{\text{FoM}} = 67$.
For comparison, the value for the 2PCF is $\sqrt{\text{FoM}} = 119$

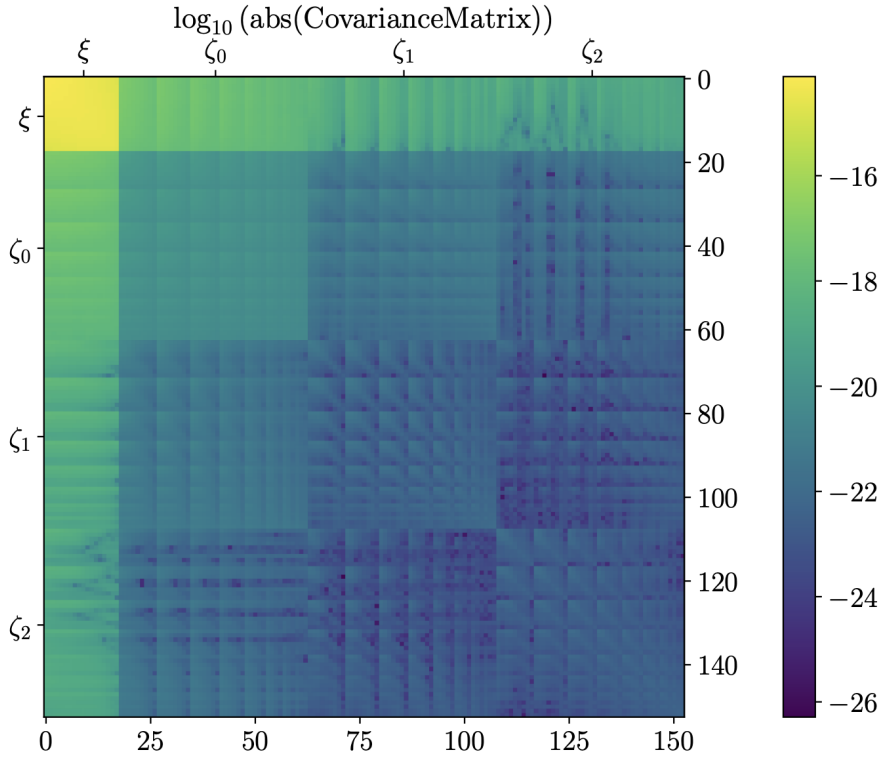
$\log_{10}$ (abs(CovarianceMatrix))
ξ
ζ_0
ζ_1
ζ_2
0
20
40
60
80
100
120
140
0
25
50
75
100
125
150
−16
−18
−20
−22
−24
−26

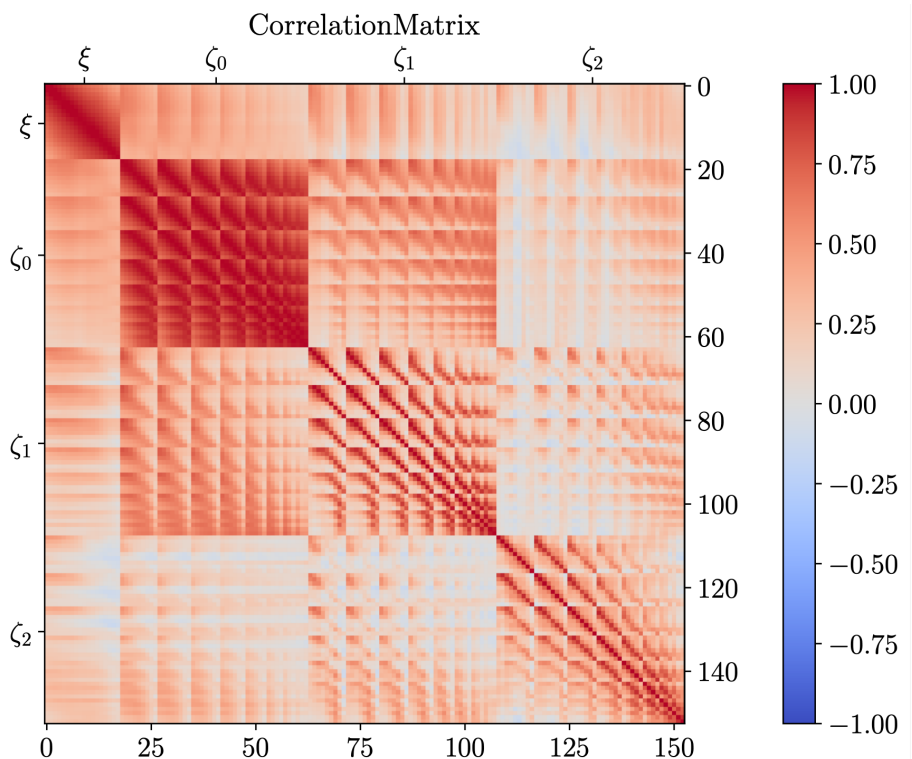
CorrelationMatrix
ξ
ζ_0
ζ_1
ζ_2
0
20
40
60
80
100
120
140
0
25
50
75
100
125
150
1.00
0.75
0.50
0.25
0.00
−0.25
−0.50
−0.75
−1.00

Beyond Fisher and S_8

- Weak lensing is primarily sensitive to the amplitude of matter fluctuation.
  - This leads to a strong degeneracy between Ω_m and σ_8 in the lensing signal.
  - The parameter S_8 captures this degeneracy direction, providing a more direct and tighter constraint from lensing data.
  - Since the degeneracy in the (Ω_m, σ_8) space is non-linear, a Fisher analysis cannot capture its characteristic “flexed” shape.

Derivative Approximation for LIkelihoods (DALI)

- Fisher Analysis

$$P_F(\vec{p}) = \exp\left(-\frac{1}{2}\Delta_i \Delta_j F_{ij}\right) \qquad \Delta = \vec{p} - \vec{\tilde{p}} \longrightarrow$$ The fiducial value

- Expands a log-probability up to second derivatives of the data vector

$$G_{ijk} = \frac{\partial^2 \zeta^a}{\partial p^i \partial p^j} \frac{\partial \zeta^b}{\partial p^k} C^{-1}_{ab}$$

$$H_{ijkl} = \frac{\partial^2 \zeta^a}{\partial p^i \partial p^j} \frac{\partial^2 \zeta^b}{\partial p^k \partial p^l} C^{-1}_{ab}$$

Derivative Approximation for LIkelihoods (DALI)

We then construct the probability distribution

$$P_D(\vec{p}) = \exp\left(-\frac{1}{2}\Delta_i\Delta_j F_{ij} - \frac{1}{2}\Delta_i\Delta_j\Delta_k G_{ijk} - \frac{1}{8}\Delta_i\Delta_j\Delta_k\Delta_l H_{ijkl}\right)$$

where: $\vec{p} = (\Omega_m, \sigma_8)$

$$\Delta = \vec{p} - \vec{\tilde{p}}$$

- Transforming parameters using a linear relation

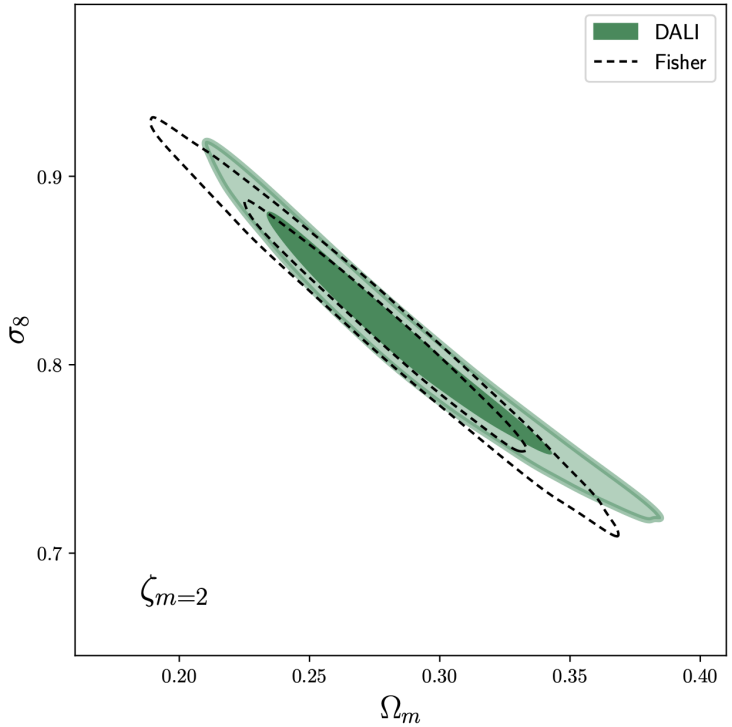
DALI
Fisher
σ_8
0.9
0.8
0.7
$\zeta_{m=2}$
0.20
0.25
0.30
0.35
0.40
Ω_m

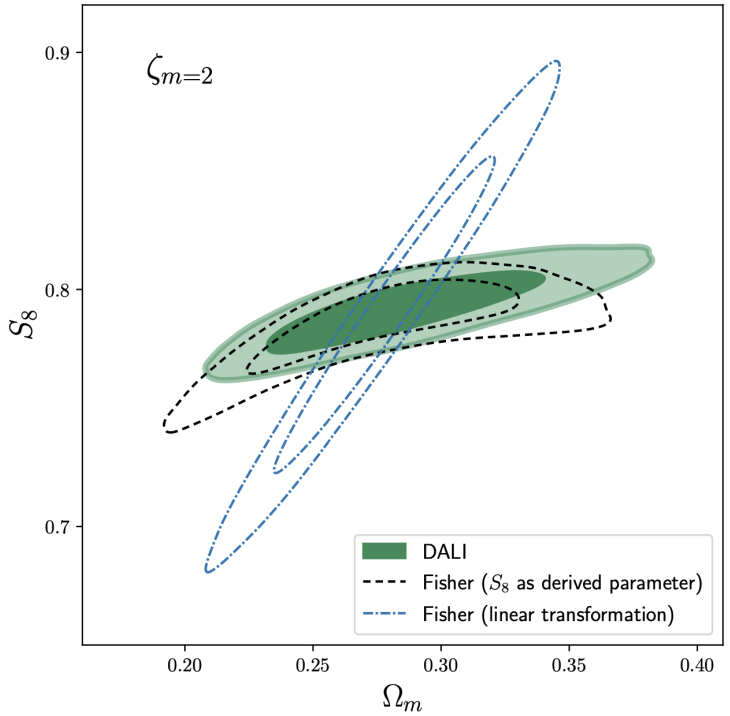
S_8
0.9
0.8
0.7
$\zeta_{m=2}$
DALI
Fisher (S_8 as derived parameter)
Fisher (linear transformation)
0.20
0.25
0.30
0.35
0.40
Ω_m

Principal Component Analysis (PCA)

- A challenge in our analysis is to estimate a reliable inverse covariance matrix that allows us to perform forecasts using high-dimensional data vectors.

$$N_{bins} = \underbrace{18}_{\text{2PCF}} + \underbrace{(9 \times 45)}_{\text{3PCF}} = 423$$

$$N_{sims} = 108$$

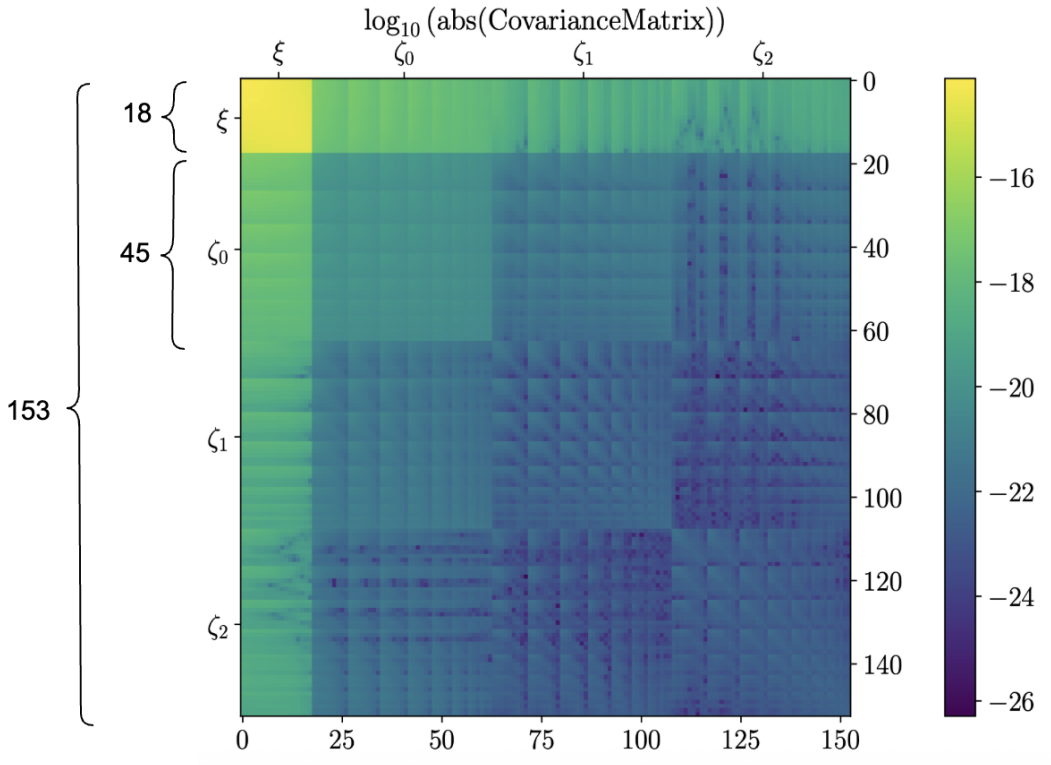

Shortcoming:

- N_{bins} is large. So the covariance is still noisy and biased, or even it can be singular.

- The data vector is highly redundant. Thus, analyzing the full data vector may be inefficient or not even possible.

- This further reduces the usefulness of treating all 423 bins and motivates a more compact representation.

Forecast with PCA

- By using a Principal Component Analysis the compressed data vector is composed of statistical independent modes and suppresses directions dominated by noise or degeneracies.

- Our purpose is to test how many components can we retain in the PCA of the 3PCF without losing cosmological information

1. Decompose the covariance matrix $\mathbf{C} = \mathbf{Q}\mathbf{\Lambda}\mathbf{Q}^T$
   a. $\mathbf{\Lambda}$ is a diagonal matrix of eigenvalues sorted in descending order.
   b. $\mathbf{Q}$ is the matrix of eigenvectors accommodated in columns.

   In our case, the last $N_{bins} + 1 - N_{sims}$ are all zero, so we are limited to a maximum of 107 components.

1. We construct a "reduced" matrix $\mathbf{Q_{red}}$ by removing from $\mathbf{Q}$ the last $N_{bins} - N_{sims}$ rows.

1. Transform each data vector from the simulations $\vec{d}_{\mathrm{PCA}} = \mathbf{Q}_{red}^T \vec{d}$

Hartlap factor

- It has a particular relevance when the number of data bins approaches the number of simulations used to estimate the covariance matrix.

$$C^{-1} \rightarrow \frac{N_{sims} - N_{bins} - 2}{N_{sims} - 1} C^{-1}$$

We construct the final PCA compressed data vector by including

- 18 bins from the 2PCF
- For the transformation matrix $\mathbf{Q}_{PCA}$ we used the first 38 eigenvectors of the sample covariance matrix

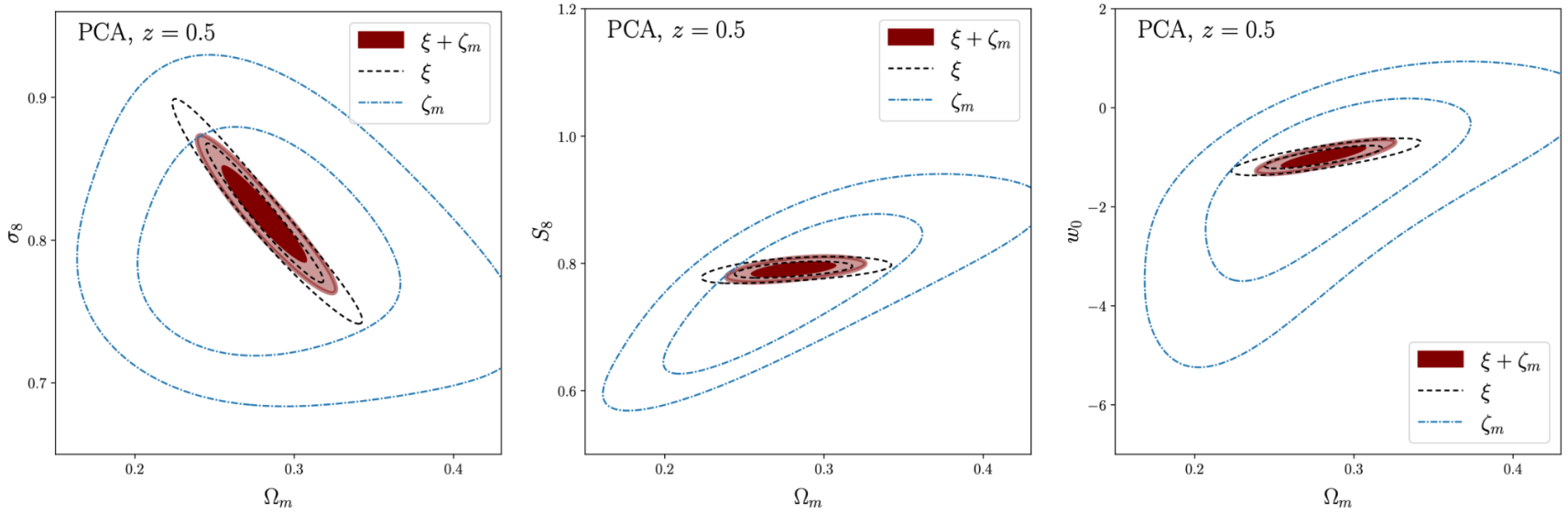

Taking into account that we use a compressed data vector with 38 bins, and a suite of 108 simulations.
This gives a simulation-to-bin ratio of 2.84 and a Hartlap correction factor of 0.65.

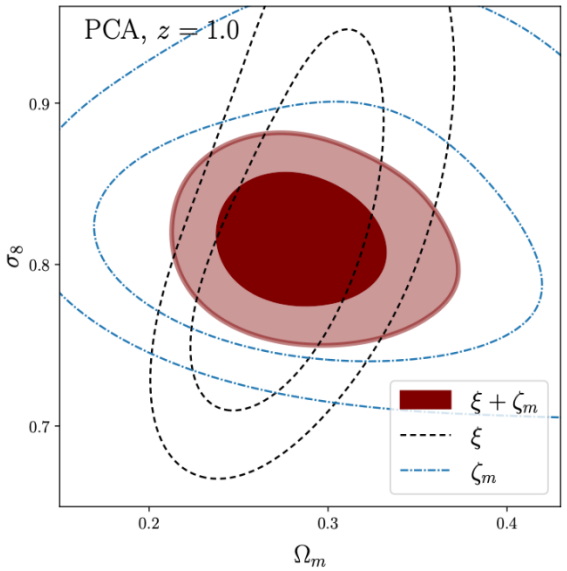
PCA, $z = 1.0$
σ_8
Ω_m
$\xi + \zeta_m$
ξ
ζ_m

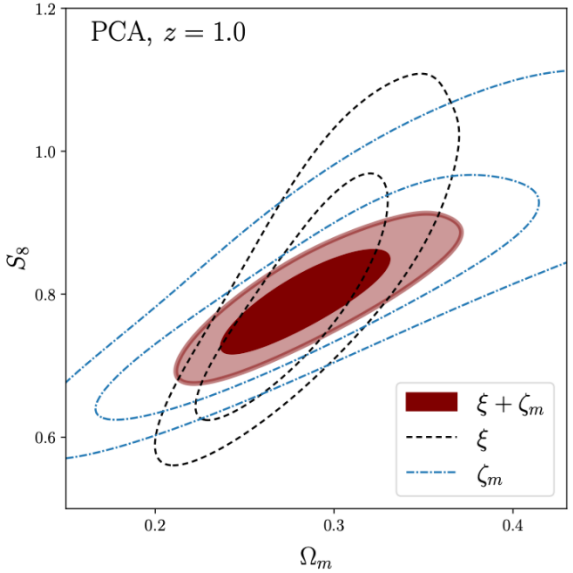
PCA, $z = 1.0$
S_8
Ω_m
$\xi + \zeta_m$
ξ
ζ_m

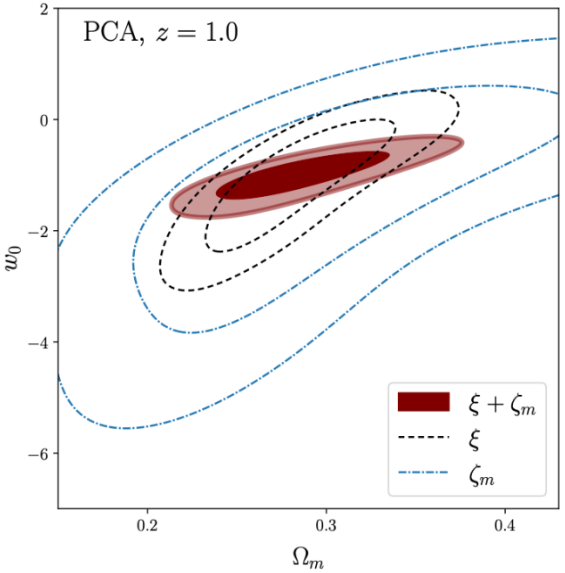
PCA, $z = 1.0$
w_0
Ω_m
$\xi + \zeta_m$
ξ
ζ_m

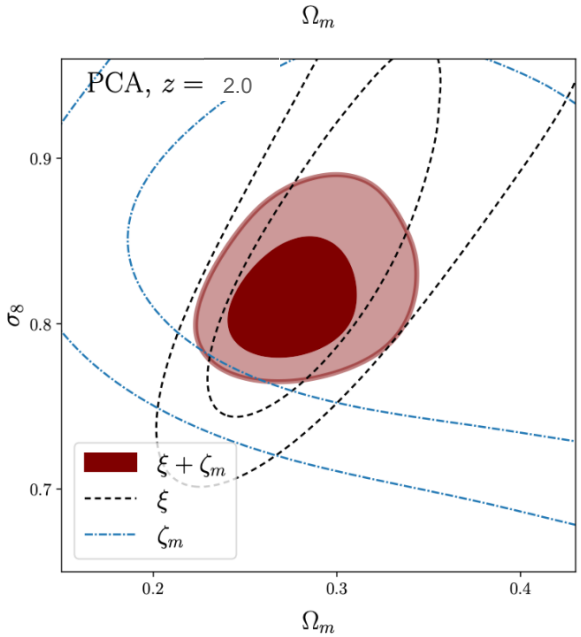
Ω_m
PCA, $z =$ 2.0
σ_8
0.9
0.8
0.7
0.2
0.3
0.4
Ω_m
$\xi + \zeta_m$
ξ
ζ_m

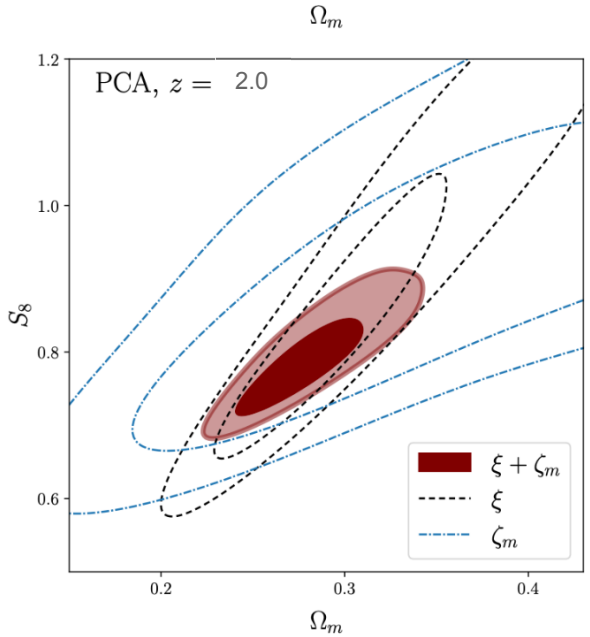
Ω_m
PCA, $z =$ 2.0
S_8
1.2
1.0
0.8
0.6
0.2
0.3
0.4
Ω_m
$\xi + \zeta_m$
ξ
ζ_m

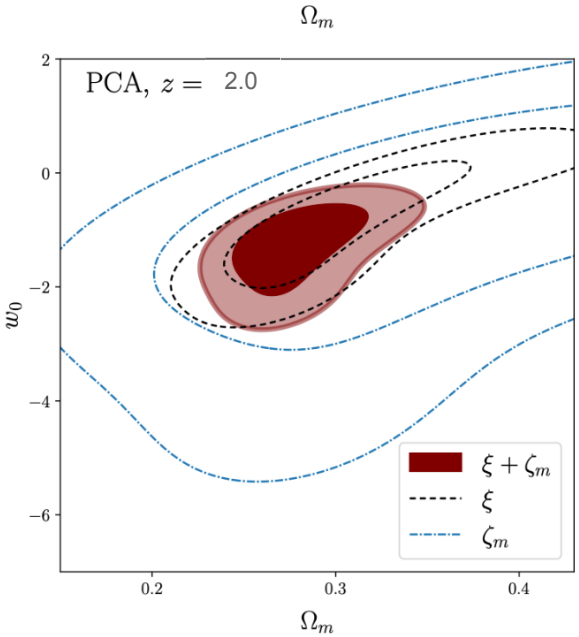
Ω_m
PCA, $z =$ 2.0
w_0
2
0
−2
−4
−6
0.2
0.3
0.4
Ω_m
$\xi + \zeta_m$
ξ
ζ_m

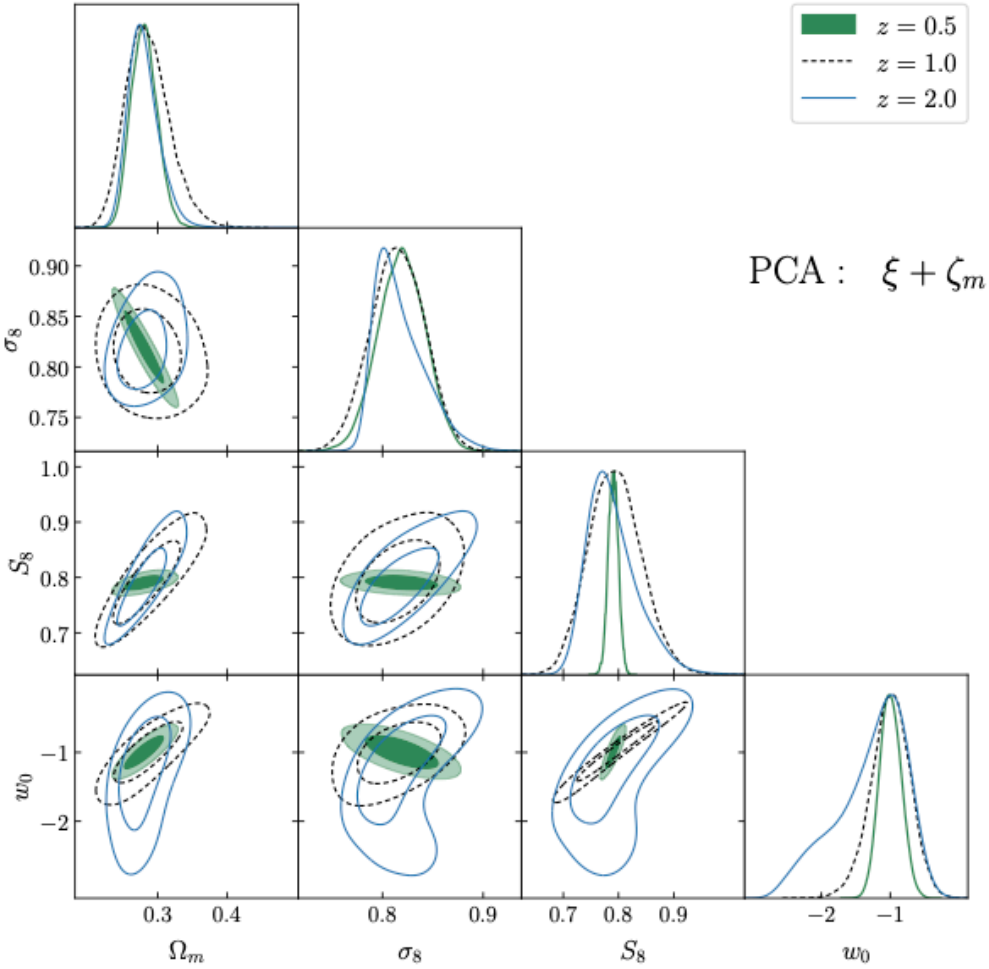
$z = 0.5$
$z = 1.0$
$z = 2.0$
PCA : $\xi + \zeta_m$
Ω_m
σ_8
S_8
w_0

Gaussian Analytical Covariance

$$\mathrm{C} = \langle \hat{\zeta}(\vec{\theta}_1, \vec{\theta}_2, \vec{\theta}_3)\hat{\zeta}(\vec{\theta}'_1, \vec{\theta}'_2, \vec{\theta}'_3)\rangle - \langle \zeta(\vec{\theta}_1, \vec{\theta}_2, \vec{\theta}_3)\rangle\langle \zeta(\vec{\theta}'_1, \vec{\theta}'_2, \vec{\theta}'_3)\rangle$$

$$= \langle \kappa_1\kappa_2\kappa_3\kappa'_1\kappa'_2\kappa'_3\rangle - \langle \kappa_1\kappa_2\kappa_3\rangle\langle \kappa'_1\kappa'_2\kappa'_3\rangle$$

$$= \langle \kappa_1\rangle\langle \kappa_2\kappa_3\kappa'_1\kappa'_2\kappa'_3\rangle + \ldots . (5\text{Terms})$$

$$+\langle \kappa_1\kappa_2\rangle\langle \kappa_3\kappa'_1\kappa'_2\kappa'_3\rangle + \ldots (4\text{Terms})$$

$$+\langle \kappa_1\kappa_2\kappa'_3\rangle\langle \kappa'_1\kappa'_2\kappa_3\rangle + \ldots . (8\text{Terms})$$

$$+\langle \kappa_1\kappa_2\rangle\langle \kappa_3\kappa'_1\rangle\langle \kappa'_2\kappa'_3\rangle + \ldots . (14\text{Terms})$$

Gaussian part

$$C_{mm'} = \frac{1}{(2\pi)^4}\int d\phi_1 d\phi_2 d\phi_1' d\phi_2' \langle \hat{\xi}(\vec{\theta}_1, \vec{\theta}_2)\hat{\xi}(\vec{\theta}_1', \vec{\theta}_2')\rangle e^{-im\phi} e^{-im'\phi'}$$

$$= \frac{1}{2f_{sky}}\int_0^\infty r dr \Big\{ \xi_+(r)[f_{m,m'}(r;\theta_1,\theta_1')f_{m,m'}(r;\theta_2,\theta_2') + f_{m,m'}(r;\theta_1,\theta_2')f_{m,m'}(r;\theta_2,\theta_1')] + f_m(r;\theta_2)f_{m,m'}(r;\theta_1,\theta_1')f_{m'}(r;\theta_2')$$

$$+ f_m(r;\theta_2)f_{m,-m'}(r;\theta_1,\theta_2')f_{m'}(r;\theta_1') + f_m(r;\theta_1)f_{m,m'}(r;\theta_2,\theta_2')f_{m'}(r;\theta_1') + f_m(r;\theta_1)f_{m,-m'}(r;\theta_2,\theta_1')f_{m'}(r;\theta_2') \Big\}.$$

$$\xi_+(r) = \frac{1}{2\pi}\int d\ell_3 \ell_3 C(\ell_3) J_0(r\ell_3), \qquad f_m(r;c) = \frac{1}{2\pi}\int d\ell\, \ell C(\ell) J_m(\ell c) J_m(r\ell)$$

$$f_{m,m'}(r;\theta_i,\theta_j') = \frac{1}{2\pi}\int d\ell\, \ell C(\ell) J_m(\ell\theta_i) J_{m'}(\ell\theta_j') J_{m+m'}(r\ell)$$

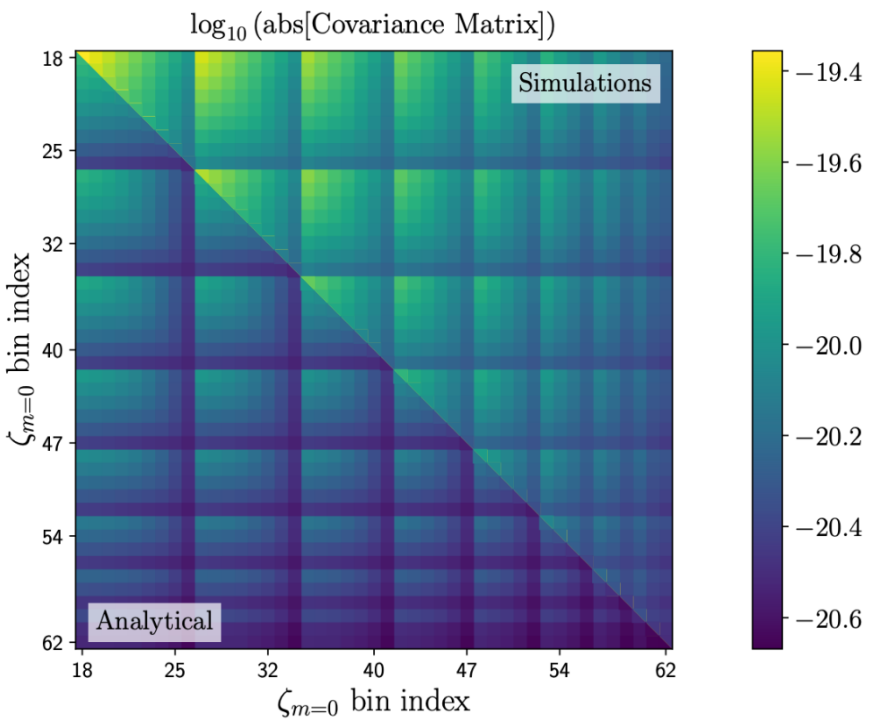
log10 (abs[Covariance Matrix])
Simulations
Analytical
18
25
32
40
47
54
62
ζm=0 bin index
ζm=0 bin index
−19.4
−19.6
−19.8
−20.0
−20.2
−20.4
−20.6

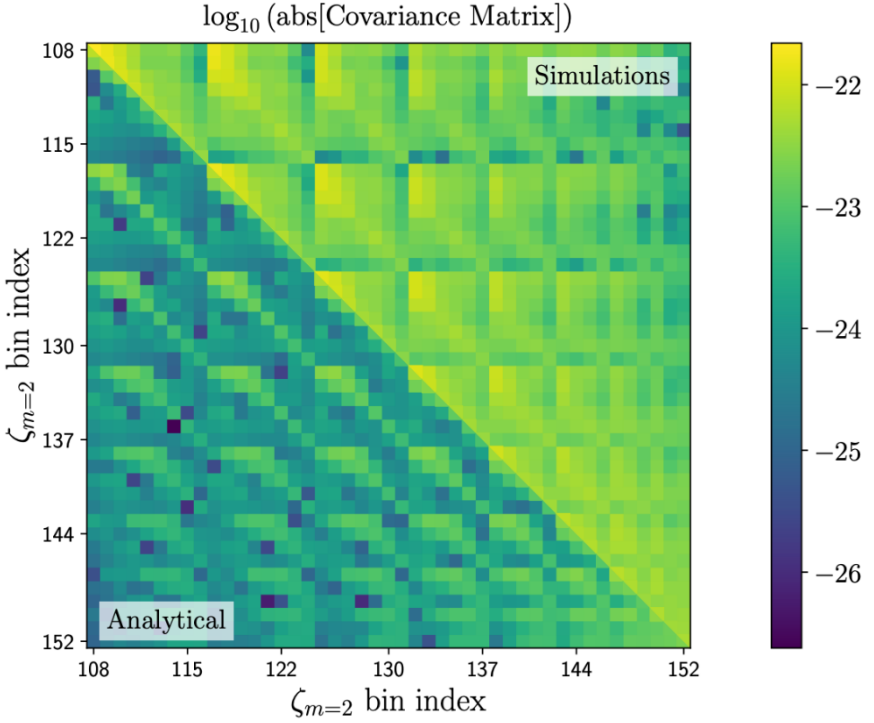
log10 (abs[Covariance Matrix])
Simulations
Analytical
108
115
122
130
137
144
152
ζm=2 bin index
ζm=2 bin index
−22
−23
−24
−25
−26

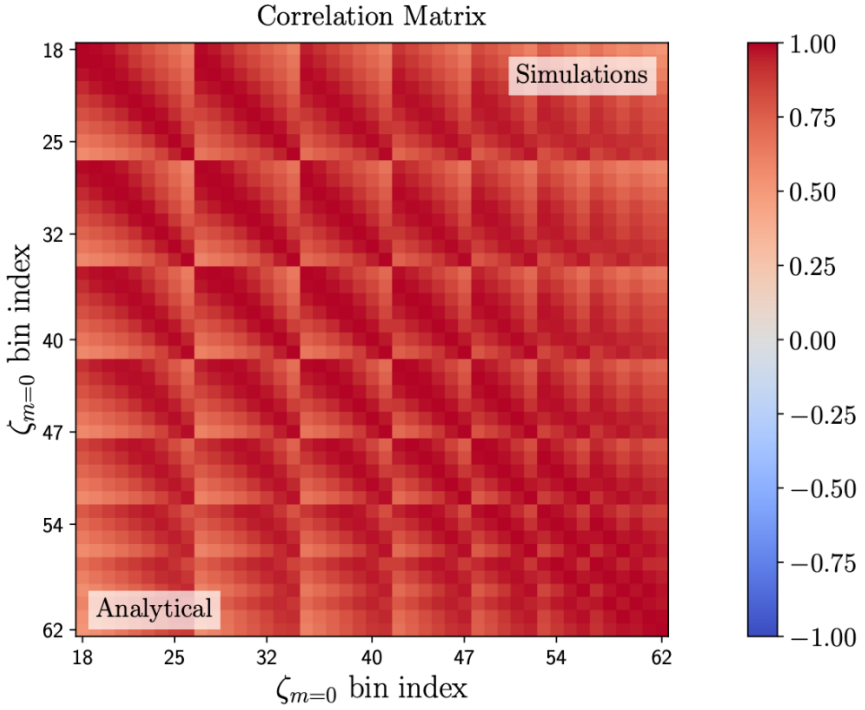
Correlation Matrix
Simulations
Analytical
18
25
32
40
47
54
62
$\zeta_{m=0}$ bin index
$\zeta_{m=0}$ bin index
1.00
0.75
0.50
0.25
0.00
−0.25
−0.50
−0.75
−1.00

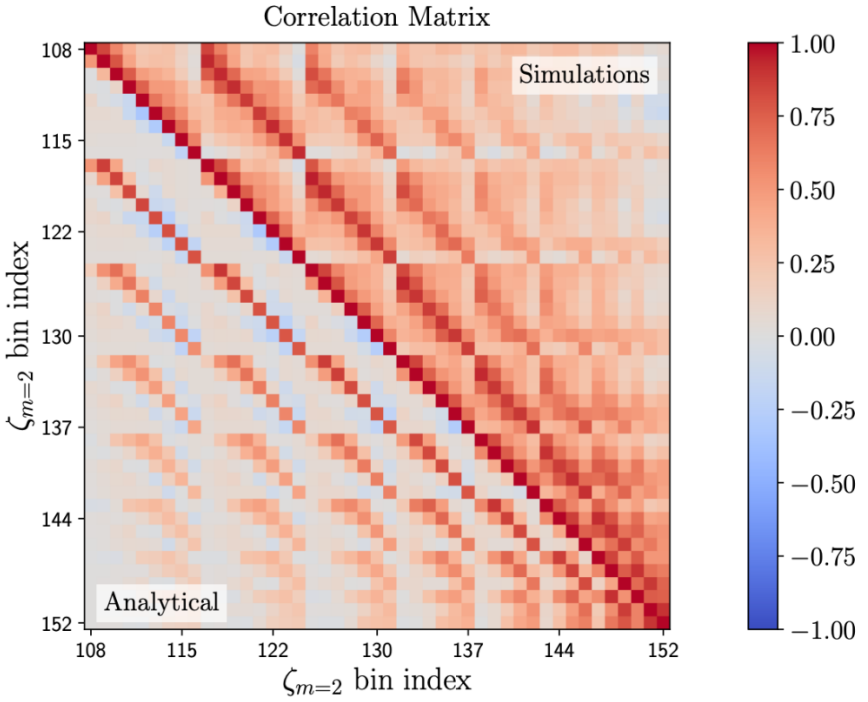
Correlation Matrix
Simulations
Analytical
108
115
122
130
137
144
152
$\zeta_{m=2}$ bin index
$\zeta_{m=2}$ bin index
1.00
0.75
0.50
0.25
0.00
−0.25
−0.50
−0.75
−1.00

- For the monopole, the differences between theory and simulations arise mainly as a normalization factor, which changes smoothly from about 0.4 at small angles to 0.8 at large angles, where the Gaussian prescription underestimates the sample covariance.

- For the quadrupole, the differences are more pronounced, not only in normalization factors, but also in the overall patterns, which are less consistent compared to the monopole case. Further, the upper-right panel shows that noise becomes more significant in the quadrupole

Conclusions

- We show that only the first four multipoles, are sufficient to extract most of the cosmological information available from the 3PCF.

- We find that the 3PCF improves the constraint on Ω_m and σ_8 by nearly 20% compared to constraints when using only the 2PCF.

- We find no significant improvements for parameters S_8 and w_0 for redshift $z = 0.5$. However, at $z = 1.0$ and $z = 2.0$, and despite obtaining weaker overall constraints, we observe considerable improvements in the parameters S_8 and w_0.

Conclusions

- We conclude that the improved constraining power originates from Ω_m and it is transferred to other parameters through their degeneracies.

- The results, coming from the gaussian matrix, substantially underestimate the errors. Nevertheless, we consider that this analysis can serve as a basis for hybrid, semi-analytical constructions of covariance matrices based on theory and simulations.

Thanks for your attention!

:)